Enzymatic Transition State Poise and Transition State Analogues

VERN L. SCHRAMM*

Department of Biochemistry, Albert Einstein College of Medicine, 1300 Morris Park Avenue, Bronx, New York 10461

Received October 23, 2002

ABSTRACT

The development of kinetic isotope effect methods for enzymatic reactions has resulted in the systematic determination of enzymatic transition state structure for several distinct chemical reaction mechanisms. Although it is early in the experimental development of the method, examples of concerted nucleophilic displacements (A_ND_N or S_N2), aromatic nucleophilic displacements (A_N*D_N or S_NAr), and both concerted and stepwise dissociative nucleophilic displacements (D_NA_N and D_N*A_N; S_N1 reactions) have been exemplified. The transition state for each reaction exhibits a characteristic extent of bond-breaking and bond-making, defined here as transition state poise. Thus, concerted nucleophilic displacements (S_N2 or D_NA_N) exhibit various extents of residual bond order to the leaving group and to the attacking nucleophile at the transition state. Aromatic nucleophilic displacements reach their rate-limiting transition states before or after formation of the tetrahedral intermediate. Several concerted, symmetric nucleophilic displacements at carbon have been described. Enzymatic transition state poise is summarized in a single diagram of bond orders using the terminology of Jencks. The analysis reveals enzymatic contributions to transition state poise, provides precedent for assignment of reaction types, and summarizes the current status of the experimental characterization of enzymatic transition states. Binding strengths of transition state analogues are readily correlated with transition state poise.

I. Introduction

Kinetic isotope effects (KIEs) are the change in reaction rates caused by an isotopic substitution.[1] Kinetic isotope effects provide transition state information for enzymatic reactions when making or breaking covalent bonds are slow steps in the reaction, or when corrections can be made for interfering steps.[2,3] Fortunately, methods have been established to reveal intrinsic KIEs by use of altered pH, temperature, sub-optimal substrates, mutated enzymes, substrate trapping experiments, and rapid reaction techniques.[4] Bond-energy bond-order vibrational analysis (BEBOVIB), and its successors (VIBE, ISOEFF, and CTBI) that incorporate quantum chemical calculations, provide practical, but still-evolving approaches for the conversion of experimental KIE to transition state information.[5−9]

The challenges of producing substrates labeled with isotopes have been largely overcome by improved chemoenzymatic methods of synthesis for labeled substrates, now in demand for KIE studies as well as for NMR and vibrational spectroscopy.[4,10−11] The accurate measurement of small KIEs has been solved by competitive label methods and advances in mass spectrometry and NMR.[12−14]

Early analyses of enzymatic transition states used two isotope effects to establish the oxacarbenium character of a transition state for lysozyme.[15] More extensive studies on catechol-O-methyl transferase included transition state mapping to establish the Pauling bond order to attacking and departing nucleophiles.[16] Current analyses of enzymatic transition states measure KIE for many positions in the same substrate to provide bond information for all reacting atoms and their neighbors at the transition state.[4]

Transition state analyses have established that enzymatic reactions differ from their uncatalyzed counterparts, and even isozymes have altered transition state structures specified by catalytic site environments. This observation is related to the well-known influence of solvent on transition state structure.[17] In enzymatic reactions, the solvent for transition state formation is the interior cavity of the catalytic site. During catalysis, the active site is closed, bulk solvent is excluded, and substrate escape is highly improbable, equivalent to the statements that enzymes bind tightly to the transition state complex or stabilize the transition state structure. However, other views have been published.[18]

Here, we describe the extent of bond-breaking and bond-making at the transition states of enzymatic nucleophilic displacements as transition state poise. Examples are provided from the steadily accumulating information of experimentally established enzymatic transition states. Chemically stable analogues of enzymatic transition states are powerful inhibitors, and their design depends critically on transition state poise and the enzymatic contacts that generate the transition state. It is possible to design transition state analogues that are isozyme-specific and therefore tissue- or species-specific. Several examples of isozyme specificity in inhibitor design are already well established, including inhibitors with specificity for mammalian or bacterial dihydrofolate reductases,[19] and others are discussed below. Finally, determination of enzymatic transition states is essential for the field of computational enzymology.

II. Transition State Poise for Enzymatic Reactions

Enzymatic transition states have now been experimentally established for most chemically accessible regions of the More O'Farrell−Jencks reaction diagram (Figure 1). This distribution of enzymatic transition states illustrates that transition state analysis for enzymatic reactions is not restricted by reaction type. The upper left corner of the

Vern L. Schramm received his Ph.D. degree with John Morrison at the Australian National University, John Curtain School of Medical Research, in 1968. In the Department of Biochemistry at the Temple University School of Medicine, he applied kinetic isotope effects to the study of enzymatic transition states (1971−1987). At the Albert Einstein College of Medicine since 1987, he has developed a systematic program of solving enzymatic transition states by kinetic isotope effects. Focus on enzymatic transition states has provided novel insights into the nature of enzymatic catalysis and has provided the most powerful inhibitors known for the N-ribosyltransferases. One inhibitor, Immucillin-H, is currently in clinical trials.

* Telephone: 718-430-2813. Fax: 718-430-8565. E-mail: vern@aecom.yu.edu.

10.1021/ar0200495 CCC: $25.00
Published on Web 05/08/2003

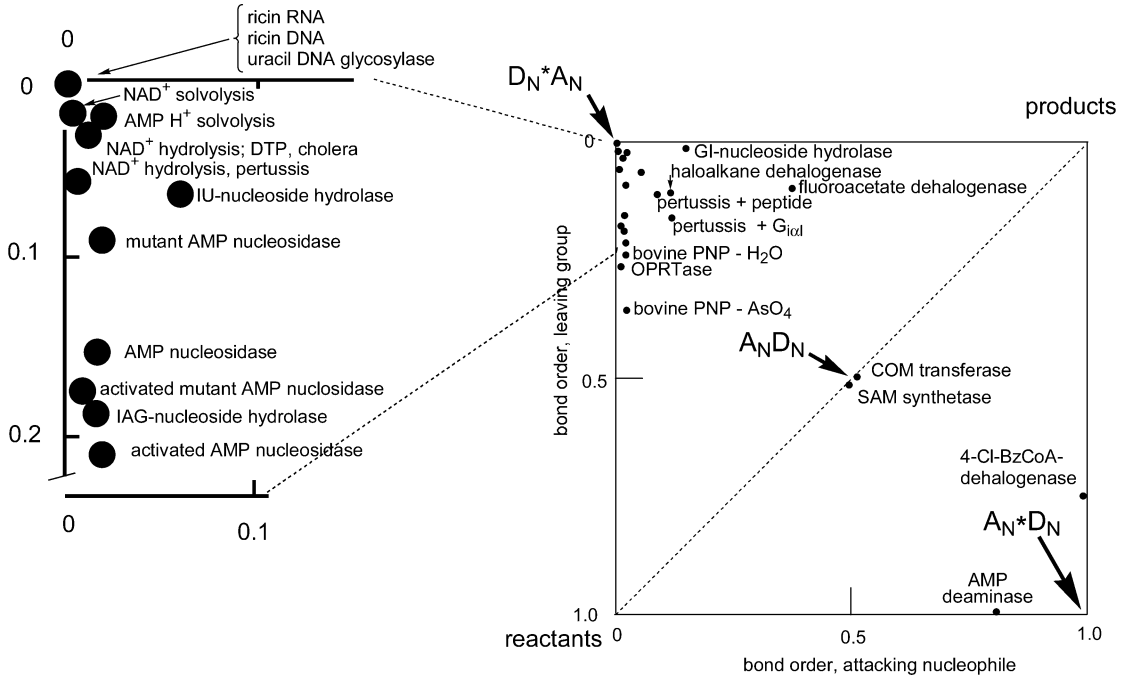

FIGURE 1. Transition state poise for enzymatic reactions. Bond orders for A_ND_N transition states with large mass differences between attacking and leaving groups are given as reduced mass.[54] Reactions with intermediates (A_N*D_N) have two transition states, and the bond orders are for the transition state giving rise to isotope effects (the highest energetic barrier). Primary references are indicated in the text or in the reference list.[55–57]

diagram describes enzymatic reactions with dissociative transition states. At present, many of these examples are N-ribosyl transferases, in which the transition states are characterized by ribooxacarbenium ion character of differing degrees, with varied bond order remaining to the leaving group and different extents of participation of the incipient nucleophile. Glucosidases also belong in this corner; however, more information is needed to permit accurate determination of bond orders at their transition states. Near the center of the diagram are symmetric nucleophilic displacements, catalyzed by catechol-O-methyltransferase and S-adenosylmethionine synthetase. These nucleophilic displacements at carbon are characterized by large KIE at the central carbon and small secondary KIE. In the lower right corner are examples of enzymatic transition states solved for nucleophilic aromatic substitutions. In the enzymatic deamination of AMP, the catalytic site Zn^{2+} converts a water to the hydroxyl nucleophile, and the highest-barrier transition state is reached at 0.8 bond order to the attacking nucleophile.[20] The subsequent formation of the Meisenheimer tetrahedral intermediate and its protonation are energetically favorable relative to formation of the first transition state. Decomposition of this complex by loss of NH_3 introduces an irreversible step; thus, only the chemical steps prior to deamination are observed in the KIE. Reactions with stable intermediates are characterized by two transition states, and the kinetic isotope effects report on the slowest step. In the 4-chlorobenzyl-CoA dehalogenase, the transition state observed by KIE is decomposition, rather than formation of the covalent intermediate.[21]

III. D_N*A_N Transition States and Analogues as Inhibitors

Enzymatic nucleophilic displacements with fully dissociated and enzyme-stabilized ribooxacarbenium ion intermediates include the transition states of ricin A-chain acting on small stem-loop RNA and DNA substrates and uracil DNA glycosylase acting on a minimal substrate (Figure 1).[22,23] Ricin A-chain depurinates a specific adenine (G*A*GA) in a four-base RNA hairpin loop from 28s ribosomal RNA, causing it to be a powerful cytotoxin. These reactions have a fully dissociated ribooxacarbenium ion intermediate, with a nonchemical step separating the two transition states. The chemically similar hydrolytic excision of uracil from DNA by uracil DNA glycosylase removes uracil errors from DNA in the first step of DNA repair. On the basis of the similarity of KIE values between uracil DNA glycosylase and those from ricin A-chain, the transition state of the DNA glycosylase was also determined to be an enzyme-stabilized deoxyribooxacarbenium ion.[24] The lifetimes of sugar oxacarbenium ions in water are estimated to be 10^{-12} s, prohibiting the formation of fully developed ribooxacarbenium ions for nonenzymatic reactions in nucleophilic solvents.[25] These transition states require that the catalytic site environments protect the oxacarbenium ions from solvent. Shielding of the intermediate from solvent has been directly demonstrated in ricin A-chain by mixtures of methanol in the solvent. Exposure of a developing ribooxacarbenium ion to this nucleophile would result in a methoxy adduct. None is found in the ricin reaction, consistent with a transition state environment that fully shields the ribooxacarbenium ion.[22] There are no crystal structures of ricin A-chain with

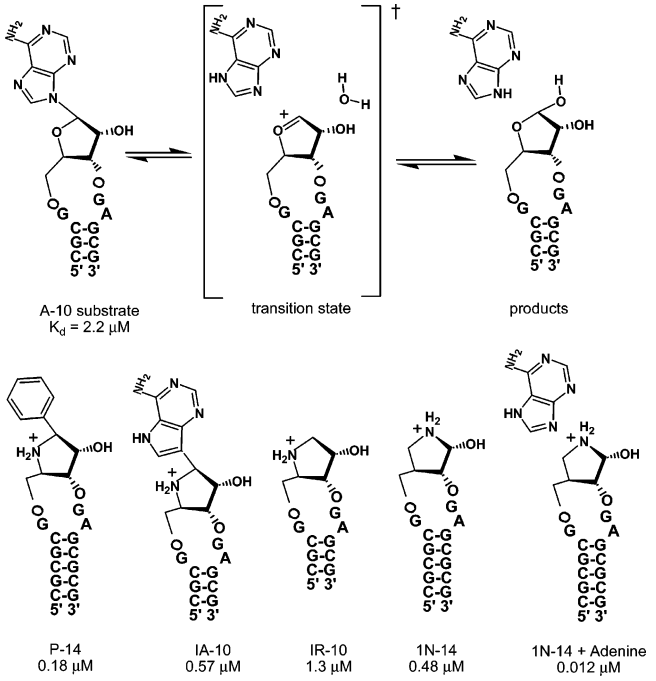

FIGURE 2. Reaction catalyzed by ricin A-chain and some analogues of the transition state. The two transition states are closely related to the oxacarbenium ion intermediate.

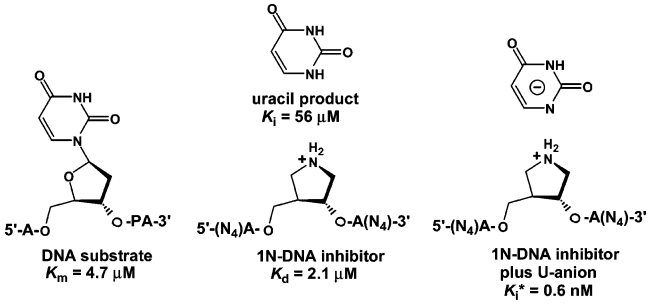

FIGURE 3. Substrate and transition state analogues for uracil DNA glycosylase.

bound RNA, but for uracil DNA glycosylase in complex with a substrate analogue, a catalytic site water nucleophile is sequestered from solvent and located 3.6 Å from the anomeric carbon. Transition state formation is preceded by the departure of uracil, leaving both the uracil N1 and the water with no significant bond order to the ribosyl anomeric carbon when the transition state is reached. The reaction coordinate is completed by translation of the anomeric C-1′ carbon and the water toward each other to form the products.[26]

The binding of transition state analogues to these enzymes provides supporting evidence for the dissociative nature of the transition states. Substrates for ricin A-chain include RNA stem-loop structures containing the required GAGA tertaloop, where the first A is hydrolyzed to form an apurinic site (Figure 2). Chemically stable analogues, IA-10 and P-14, mimic a D_NA_N (concerted) transition state and have been tested as inhibitors. Substrate RNA (A-10) binds with a dissociation constant of 2 μM, while the phenyl-iminoribitol (P-14) and the 9-deazaadenine-iminoribitol (IA-10) derivatives bind with K_d values of 0.18 and 0.57 μM, respectively.[27,28] Although bound more tightly than substrate, these analogues are poor transition state analogues because they incorporate covalent bonds, while the transition states have fully dissociated leaving groups. Analogues of a fully dissociated cationic transition state are IR-10 and 1N-14, but these have no purine to fill the leaving group pocket (Figure 2). The dissociation constants of 1.3 and 0.48 μM are similar to analogues with covalent bonds to the leaving groups. An improved approximation of the transition state includes the fully dissociated oxacarbenium ion mimic with a fully dissociated leaving group. The combination of 1N-14 and adenine gave the best inhibition yet reported for ricin A-chain, a K_d of 12 nM for 1N-14 with saturating adenine. Enhanced binding of transition state analogue fragments suggests components to reconstitute the dissociated transition state. Wolfenden has dissected transition state analogues of adenosine deaminase with the conclusion that 7−10 kcal/mol can be gained from the appropriate connectivity of fragments of transition state analogues.[29] The complementary binding of ricin A-chain transition state components supports a transition state closely resembling the fully dissociated carbocation intermediate.

A fully dissociated oxacarbenium intermediate for ricin A-chain requires that the enzyme be able to effect separation and stabilization of three components, the adenine leaving group, the ribooxacarbenium ion, and the incipient water nucleophile. Separation is assisted if the ion pair normally formed by loss of adenine (as an anion) from a ribosyl center (to form a cation) can be made neutral at the transition state. Proton donation from the enzyme to the adenine leaving group accomplishes leaving group activation. An indication of strong interactions with the leaving group comes from the lack of substrate activity using *p*-nitrophenyl-β-D-riboside in a stem-loop RNA to replace the adenylate group of the substrate (Figure 2). Enzymes that act primarily by ribooxacarbenium ion formation without strong leaving group activation can use substrates with a variety of good leaving groups.[30] Thus, substrate specificity and transition state interactions in ricin A-chain involve specific interactions with the adenine leaving group.

Uracil DNA glycosylase recognizes sites in double-stranded DNA that contain uracil mutations and cause local denaturation to flip the uracil from the base-paired structure, enclose it into the catalytic site of the enzyme, and hydrolyze it to initiate subsequent repair steps (Figure 3).[31] Inhibitor specificity for uracil DNA-glycosylate is also consistent with a fully dissociated transition state. Thus, the minimal DNA substrates modified to incorporate the 1-aza mimic of the 2-deoxyribose oxacarbenium ion gave a dissociation constant of 2 μM alone, but when the uracil anion was also added, the dissociation constant decreased to 0.6 nM, the highest affinity complex reported for this enzyme.[32]

IV. Transition State Structure and Analogues for Isozymes of Nucleoside Hydrolases

Nucleoside hydrolases (NH) are protozoan and bacterial enzymes involved in base salvage and recycling, the methionine salvage pathway and bacterial quorum sensing.[33−35] Transition state structures have been solved for three nucleoside hydrolase isozymes (Figure 1).[36] (KIE values for IU-NH, GI-NH, and IAG-NH have been analyzed by CTBI and the transition states analyzed. The values shown in Figure 1 vary significantly from the original bond-interpolation method used for IU-NH. Unpublished results of D. W. Parkin, P. Berti, A. A. Sauve, R. W. Miles, and V. L. Schramm, 2003. The CTBI method is described in ref 9.) All accept inosine as substrate, but demonstrate variable specificity for other nucleosides. The IU- and IAG-NHs have been characterized for inhibition by transition state analogues. Catalytic turnover for IU- and IAG-NH with inosine is 28 and 34 s^{-1}, and both use a tightly bound Ca^{2+} ion to activate and direct the water nucleophile. Transition states for IU-NH and IAG-NH indicate that more bond order remains to the leaving group purine at the transition state of IAG- than for IU-NH, establishing an earlier transition state for IAG-NH (Figure 1). This difference in transition state poise has been attributed to differences in leaving group interactions such that the IAG-NH obtains more of its catalytic activation from leaving group interactions than does IU-NH, thereby causing IAG-NH to reach the transition state with more bond order to the leaving group.[37] Bond order to the attacking nucleophile is low for the transition state of IAG-NH, but for IU-NH, the attacking nucleophile is more involved. IU-NH obtains most of its catalytic activation from conversion of the ribosyl group to the ribooxacarbenium ion, and this interaction is the dominant character of the transition state. As the oxacarbenium ion develops, a symmetric transition state is reached when the bond-order to the relatively unactivated leaving group drops to approximately 0.06 and the Ca^{2+}-bound water nucleophile also has a 0.06 bond order. The transition state of IAG-NH contrasts considerably since strong leaving group interaction causes achievement of the transition state when 0.18 bond order is remaining and only 0.02 bond order is formed to the attacking nucleophile.

Quantitation of leaving-group versus ribooxacarbenium activation energetics to reach the transition states of N-ribohydrolases was established by the use of *p*-nitrophenyl-β-D-ribose (pNPR) as substrate.[30] Hydrolysis of pNPR by IU-NH has an 8-fold increased k_{cat} relative to inosine. In contrast, hydrolysis of pNPR by IAG-NH is at 0.5% of the rate with inosine as substrate.[38] NHs can provide no activation to the *p*-nitrophenyl group; thus, the reaction rate reflects the enzyme's contribution to form the ribooxacarbenium ion. Catalytic activation for hydrolysis of inosine by these enzymes is 17.7 kcal/mol, and IU- and IAG-NHs apply 4.6 and 8.8 kcal/mol to purine departure with the remaining 13.1 and 8.9 kcal/mol applied to ribooxacarbenium ion formation (Figure 4).

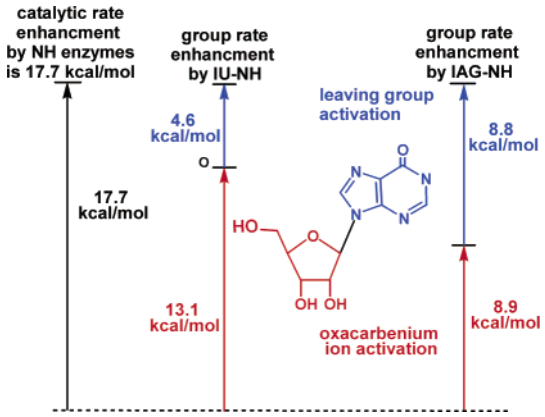

FIGURE 4. Transition state energetics for the IU- and IAG-NH isozymes. *p*-Nitrophenyl-β-D-ribofuranoside was used to quantitate energetics of ribooxacarbenium ion formation and the remaining energy of activation comes from leaving group interactions with inosine.

Isozyme-specific features of the NH transition states can be used to design specific transition state analogue inhibitors. Inhibitors specific for IAG-NH require purine leaving group features but are less specific for the ribooxacarbenium mimic. Transition state analogues of IU-NH require close mimics of the oxacarbenium ion, but non-specific hydrophobic leaving groups are sufficient for good inhibitors (Figure 5).[37] Inhibitors specific for both IU-NH and IAG-NH use transition state features of common substrates, where optimal interactions can be designed for both leaving groups and oxacarbenium ions. Thus, Immucillin-A exhibits 7 and 0.9 nM K_i* values for IU- and IAG-NH, respectively, while 2′-deoxy analogues of the iminoribitols favor IAG-NH and nonsubstrate purine bases attached to iminoribitols favor IU-NH. These transition state analogue design principles are consistent with transition state poise, substrate specificities, and energetics of transition state formation and provide dependable blueprints for inhibitor design.

V. PNP Transition States: Arsenolysis and Hydrolysis

Purine nucleoside phosphorylase (PNP) catalyzes the phosphorolysis of the N-ribosidic bonds of 6-oxypurine nucleosides and 6-oxypurine-2′-deoxynucleosides (Figure 6). A rare human genetic deficiency of PNP demonstrates that PNP is the primary pathway from (deoxy)nucleosides to purine bases. The deficiency causes the accumulation of (deoxy)nucleoside substrates, including deoxyguanosine, while preventing the formation of uric acid in affected humans.[39] Accumulation of deoxyguanosine to micromolar levels in blood causes increased dGTP in dividing T-cells, inhibition of ribonucleotide reductase, and a specific T-cell deficiency. This metabolic anomaly is being explored for treatment of T-cell proliferative diseases.[40]

The transition state for the arsenolysis of inosine by PNP has been established for the bovine enzyme, since a high forward commitment factor with phosphate prevents

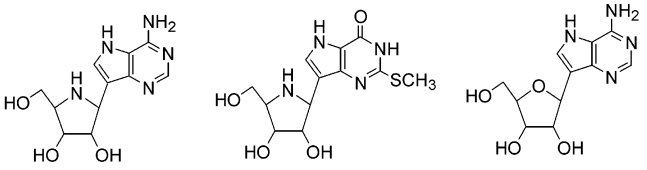

isozyme	immucillin-A	2-methylthio-immucillin-H	9-deazaadenosine
		K_d values	
IU-NH	7 nM	230 nM	1,500,000 nM
IAG-NH	0.9 nM	>50,000 nM	410 nM

FIGURE 5. Isozyme-specific transition state analogues for IU- and IAG-NH. Immucillin-A has features of both isozymic transition state structures and binds well to both. IU-NH requires ribooxacarbenium character, while IAG-NH requires features of N7 protonated purine substrates.

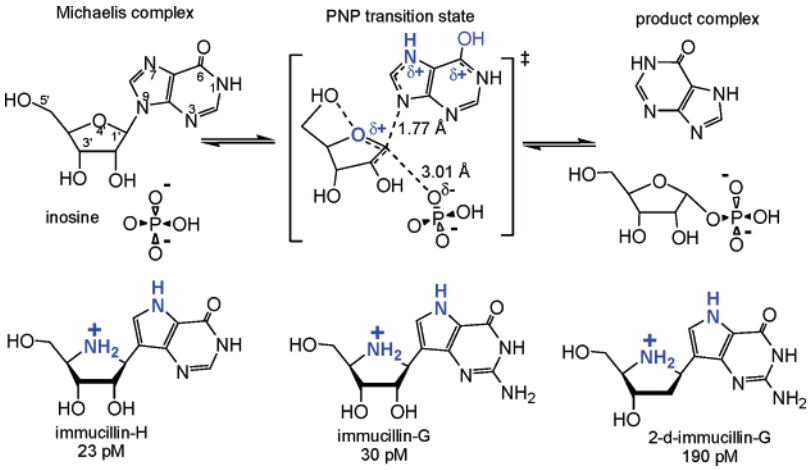

FIGURE 6. Reaction catalyzed by PNP. Three inhibitors that mimic transition state features are shown. The enzyme uses inosine, guanosine, and deoxyguanosine as substrates, making all of these transition state mimics.

expression of kinetic isotope effects.[41] Arsenate introduces a chemically irreversible step and increases the barrier height for transition state formation but gives a k_{cat} similar to that of phosphate. PNP is unusual among the N-ribosyltransferases in reaching the transition state with the largest remaining bond order to the leaving group, suggesting extraordinary leaving-group interactions with the 6-oxypurine base (Figures 1,6). These interactions are confirmed by the kinetics for the slow hydrolysis of inosine catalyzed by bovine PNP.[42] In the absence of PO_4, inosine is hydrolyzed at a single catalytic site of the homotrimer, ribose is released, and the hypoxanthine product remains bound to the enzyme with a dissociation constant of 1.3 pM—sufficient affinity to permit chromatography and stoichiometric characterization of the complex. Addition of phosphate or ribose 1-phosphate causes rapid release of the tightly bound hypoxanthine supporting a substrate-linked conformation change to effect the tight-binding. The transition state poise is determined by favorable interactions with the leaving group, activating the leaving-group to achieve transition state balance while approximately 0.36 Pauling bond order still remains in the N-ribosidic bond. This can be compared with any of theenzymatic or chemical solvolyses of N-ribosyltransferases, all of which require smaller bond orders to the leaving group to achieve transition state balance (Figure 1).

A second feature of the transition state is low bond order to the oxygen nucleophile, positioned at 3.0 Å from the anomeric carbon. Low bond order to the anionic nucleophile with approximately 0.36 bond order to the leaving group causes the ribosyl group to be electron deficient, with partial oxacarbenium character. However, even at 3.0 Å from the anomeric carbon, the anion plays a significant electrostatic role in transition state stabilization. Comparison of the transition states for the single-turnover hydrolytic reaction and that for arsenolysis reveals that the hydrolytic transition state is later. Transition state poise is indicated by the N9−C1′ bond lengths of 1.77 and 1.90 Å (bond orders of 0.36 and 0.24) for arsenolysis and hydrolysis respectively, but with no change in bond order to the nucleophile (Figure 1). Hydrolysis results from one or more waters filling the phosphate binding site, and decreases the reaction rate to 10^{-4} that of phosphorolysis. The nature of the nucleophile alters transition state poise for PNP without change in the degree of nucleophilic participation. Catalytic features causing altered transition state poise include loss of charge from the phosphate anion to stabilize an early transition state or an altered interaction of the enzyme with the purine leaving group. The release of tightly bound hypoxanthine

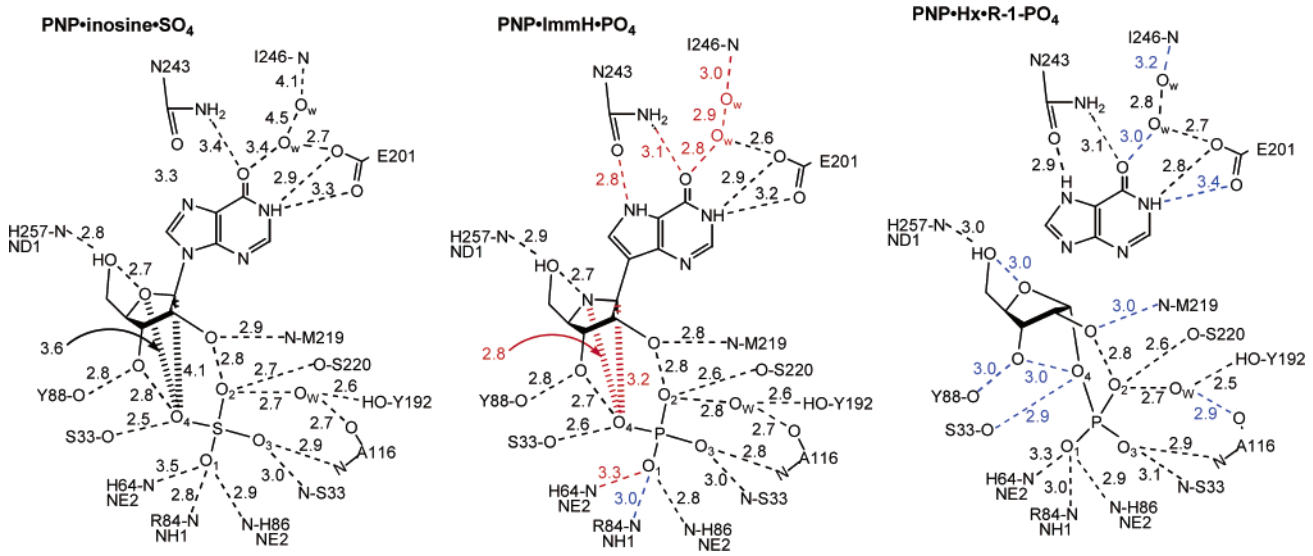

FIGURE 7. Catalytic site contacts for bovine PNP with complexes resembling the Michaelis (PNP−inosine−SO_4), transition state (PNP−ImmH−PO_4), and product (PNP−Hx−R1P) complexes. Shorter H-bonds in the PNP•ImmH•PO_4 complex compared to PNP•inosine•SO_4 are in red, and bonds that relax in the PNP•Hx•R-1-PO_4 complex are in blue.

by phosphate (see above) confirms the connectivity between phosphate and purine binding sites.

VI. PNP Transition State Analogues and Leaving Group Effects

Transition state features for the PNP-catalyzed arsenolysis of inosine were used to design transition state analogues incorporating (1) the elevated pK_a of the purine group at the transition state, (2) the oxacarbenium ion character of the ribosyl, (3) a stable substitute for the N-ribosidic bond, and (4) accommodation for the phosphate anion site to fill with inorganic phosphate to mimic the van der Waals contact of the transition state. Immucillin-H is a slow-onset, tight binding inhibitor of bovine PNP, with a K_i value of 41 nM and a K_i* value of 23 pM (Figure 6).[43] The X-ray crystal structures of PNP have been solved with inosine and SO_4 at the catalytic site, to mimic the Michaelis complex, and with Immucillin-H and PO_4 bound to mimic the transition state. The leaving group interactions responsible for the early transition state catalyzed by PNP are revealed in the structures (Figure 7).[44] Four or five direct hydrogen bonds to the purine base and two additional hydrogen bonds in a proton-transfer bridge characterize the PNP interactions in these complexes. Enzyme−ligand distances are 3.3, 3.4, 3.4, 2.9, 3.3, 4.5, and 4.1 Å in the Michaelis complex with inosine and SO_4 and are 2.8, 3.1, 2.8, 2.9, 3.2, 2.9, and 3.0 Å in the complex with Immucillin-H and PO_4. Shortened distances in six of these seven interactions provide favorable pathways for transient proton transfer to O6 and N7 at the transition state. Protonation of purine leaving groups provides a well-documented chemical path to N-riboside solvolysis.[45] The absence of general acids in direct contact with O6 and N7 requires that proton transfer occurs from solvent to achieve the transition state. Two water molecules are in contact with O6, Glu201, and solvent to form a proton-transfer bridge for both O6 and N7. Tight binding of Immucillin-H requires a proton donor at N7 for favorable interaction with the carbonyl oxygen of Asn243. In the Michaelis complex N7 is a proton acceptor, repelling the Asn243 carbonyl until N-riboside bond loss elevates the pK_a at N7, whereupon it accepts a proton and is stabilized by the interaction with the Asn243 carbonyl. Likewise, 3-deaza-4-aza-Immucillin-H cannot form the Asn243 H-bond and binds 10.1 kcal/mol less well than ImmH (Figure 8).

The crystal structures of PNP establish that reaction coordinate motion involves migration of the anomeric carbon of ribose while phosphate and the purine remain relatively fixed.[44] Transition state stabilization at the oxacarbenium site is by neighboring groups, and no interactions are contributed directly from protein. This mechanism of transition state stabilization is in contrast to the glucosyltransferases, elegantly characterized by the Withers laboratory, in which a pair of enzymatic carboxylates stabilizes the glucooxacarbenium ion transition states and/or activates a water nucleophile.[46,47] However, migration of the anomeric carbon appears to characterize reaction coordinate motion for both N-ribosyl and glucosyltransferases.

The energetics of transition state analogue binding can be investigated by atomic substitutions in the Immucillin-H transition state analogues and provide lower-limit estimates of the energetics for interactions of the transition state.[48] Several examples are pertinent to transition state poise. The proton transfer bridge in contact with O6 is proposed to contribute to an early transition state. Altering O6 to a H-bond donor site, or to an unfavorable H-bond partner in Immucillin-A and 6-S-Immucillin-H, decreased binding energy by approximately 7 kcal/mol (Figure 8). The loss of 7 kcal/mol binding energy is unlikely to arise from a single H-bond and is interpreted to be the disruption of the H-bond pattern that provides the favorable leaving-group interactions.

inhibitor	K_d	$\Delta\Delta G^o$ binding
	pM	kcal/mol
immucillin-H	23	--
immucillin-A	2,600,000	7.0
6-S-immucillin-H	1,900,000	6.8
9-(1'-CH_2)-immucillin-H	91,000	5.0
4-aza-3-deaza-immucillin-H	422,000,000	10.1
9-deaza-inosine	2,000,000	6.8

FIGURE 8. Energetics of transition state analogue binding to bovine PNP. Altering the H-bond contacts (Figure 7) causes large changes in binding energy.

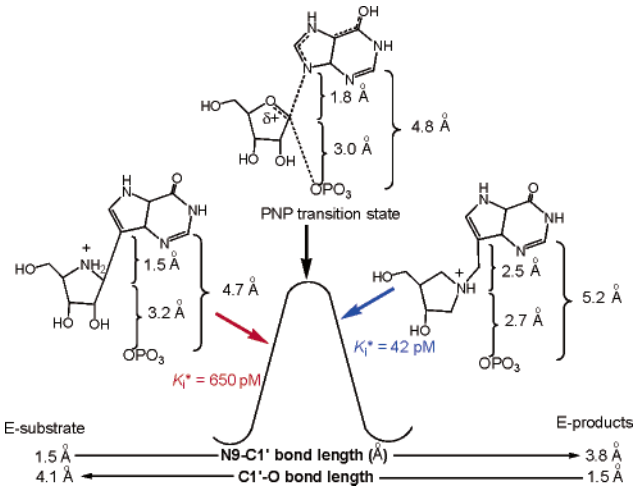

FIGURE 9. Early and late transition state analogues for PNP from *M. tuberculosis*. The methylene-bridged 42 pM inhibitor is a late transition state analogue for the phosphorolysis of deoxyinosine, a good substrate for PNP. The K_i* values shown here are for *M. tuberculosis* PNP. Geometry at the transition state is taken from the KIE analysis of the transition state with bovine PNP. Distances for both inhibitors are taken from the crystal structures of PNP from *M. tuberculosis*.[58]

Protonation of N7 also favors formation of an early transition state. In the crystal structures of PNP, there are no significant interactions at N3 of the purine ring. Inversion of N3 and C4 gives 3-deaza-4-aza-Immucillin-H, making N7 a H-bond acceptor. The loss of 10.1 kcal/mol binding energy demonstrates the cooperative nature of the leaving group H-bond partners.

The contribution of the iminoribitol group at N4′ to Immucillin-H binding was explored with 9-deazainosine. This isostere has a similar pK_a for N7 and the only alteration is the imino-group that stabilizes the phosphate and O5′ interactions. Binding of 9-deazainosine is 6.8 kcal/mol less favorable than Immucillin-H, also consistent with the loss of more than one hydrogen bond and/or ionic interaction. The ionization state of the imino group for Immucillin-H is critical in the evaluation of these interactions. Kinetic analysis and pH dependence of the initial phase of Immucillin-H binding (K_i) indicates that the initial binding of inhibitor is as the neutral species, similar to substrates. But after the slow-onset phase, the 4′-imino group of Immucillin-H is protonated to mimic the transition state.[49,50] This change accompanies a 2000-fold increase in affinity to give the K_i* value of 23 pM. The ability of Immucillins to bind as a neutral species to mimic the Michaelis complex, followed by enzyme-mediated protonation to mimic the ribooxacarbenium transition state has now been confirmed by computational and spectroscopic analyses for several N-ribosyltransferases.[49,50]

Chemically stable analogues are imperfect mimics of enzymatic transition states by virtue of their covalent nature compared to the partial bonds of the actual substrate as it reacts. A geometric map of transition state passage illustrates this for PNP from *Mycobacterium tuberculosis* (Figure 9). The effect of geometry can be explored by altering the distance between the leaving group and ribooxacarbenium mimics. Thus, 9-(1′-CH_2)-Immucillin-H expands the linear distance of the reaction coordinate by approximately 1 Å and is a poor inhibitor, while a similar change, but with the cation at the position of the anomeric carbon, makes a powerful inhibitor (Figures 8 and 9). These analogues emphasize the close match in both geometry and electrostatics required for transition state binding interactions.

VII. Transition State Poise as a Function of Attacking Nucleophile

Bacterial exotoxins often act by using NAD^+ as a substrate to ADP−ribosylate specific GTP-binding proteins (G-proteins) of mammalian cells.[51] The toxins hydrolyze NAD^+ to ADP−ribose and nicotinamide when the G-proteins are absent, thereby providing an opportunity to investigate the effect of the nucleophile on transition state structure. Pertussis toxin ADP−ribosylates a specific cysteine on an inhibitory G-protein, $G_{i\alpha 1}$. Hydrolysis gives a transition state with approximately 0.01 Pauling bond order to the water nucleophile, and this increases to approximately 0.10 when a cysteine peptide is used as substrate and to 0.15 when the $G_{i\alpha 1}$ is used as substrate.[51−53] A corresponding earlier transition state with respect to

leaving group interaction occurs in each case (Figure 1). The correct fit of the thiolate anion nucleophile from the substrate permits increased nucleophilic participation and the anionic interaction permits access to an earlier transition state.

VIII. Summary and Conclusions

Enzymatic catalytic sites provide "designer solvents" for their cognate transition states. Transition state structures established from KIE provide novel information on transition state poise. From these bond orders and angles, computational chemistry yields electrostatic maps as models for the design of transition state analogues. These principles are now well established and can be applied to generate transition state analogues for any enzymatic reaction where chemically stable mimics of the transition state can be synthesized.

Abbreviations

IU-NH, nonspecific nucleoside hydrolase; IAG-NH, purine-specific nucleoside hydrolase; GI-NH, guanosine−inosine preferring nucleoside hydrolase.

Research described here has been generously supported by the National Institutes of Health. Major contributions have been made by Drs. David Parkin, Frank Mentch, Paul Kline, Benjamin Horenstein, Johannes Scheuring, Kathleen Rising, Paul Berti, Carey Bagdassarian, and Wuxian Shi. Inhibitor synthesis by Drs. Peter Tyler, Gary Evans and Richard Furneaux at Industrial Research Ltd., New Zealand, has played an increasing role in understanding transition states.

References

(1) Melander, L.; Saunders, W. J., Jr. *Reaction Rates of Isotopic Molecules;* John Wiley and Sons: New York, 1980; pp 4−55.
(2) Cleland, W. W., O'Leary, M. H., Northrop, D. B., Eds. In *Isotope Effects on Enzyme-Catalyzed Reactions*; University Park Press: Baltimore, 1977.
(3) Northrop, D. B. The expression of isotope effects on enzyme-catalyzed reactions. *Annu. Rev. Biochem.* **1981**, *50*, 103−131.
(4) Cook, P. F., Ed. In *Enzyme Mechanism From Isotope effects*; CRC Press: Boca Raton, FL, 1991.
(5) Sims, L. B.; Lewis, D. E. Bond order methods for calculating isotope effects in organic reactions. In *Isotopes in Organic*; Buncel, E., Lee, C. C., Eds.; Elsevier: New York, 1984; Chemistry Vol. 6, pp 161−259,.
(6) Huskey, W. P. Model calculations of isotope effects using structures containing low-barrier hydrogen bonds. *J. Am. Chem. Soc.* **1996**, *118*, 1663−1668.
(7) Anisimov, V.; Paneth, P. ISOEFF98. A program for studies of isotope effects using Hessian modifications. *J. Mater. Chem.* **1999**, *26*, 75−86.
(8) Berti, P. J.; Schramm, V. L. Transition State Structure of the Solvolytic Hydrolysis of NAD^+. *J. Am. Chem. Soc.* **1997**, *119*, 12069−12078.
(9) Berti, P. J. Determining transition states from kinetic isotope effects. *Methods Enzymol.* **1999**, *308*, 355−397.
(10) Rising, K. A.; Schramm, V. L. Enzymatic synthesis of NAD^+ with the specific incorporation of atomic labels. *J. Am. Chem. Soc.* **1994**, *116*, 6531−6536.
(11) Parkin, D. W.; Leung, H. B.; Schramm, V. L. Synthesis of nucleotides with specific radiolabels in ribose. Primary ^{14}C and secondary ^{3}H kinetic isotope effects on acid-catalyzed glycosidic bond hydrolysis of AMP, dAMP and inosine. *J. Biol. Chem.* **1984**, *259*, 9411−9417.
(12) Berti, P. J.; Blanke, S. R.; Schramm, V. L. Transition state structure for the hydrolysis of NAD^+ catalyzed by diphtheria toxin. *J. Am. Chem. Soc.* **1997**, *119*, 12079−12088.
(13) Gawlita, E.; Paneth, P.; Anderson, V. E. Equilibrium isotope effect on ternary complex formation of [1-^{18}O]oxamate with NADH and lactate dehydrogenase. *Biochemistry* **1995**, *34*, 6050−6058.
(14) Keating, A. E.; Merrigan, S. R.; Singleton, D. A.; Houk, K. N. Experimental proof of the nonleast-motion cycloadditions of dichlorocarbene to alkenes: Kinetic isotope effects and quantum mechanical transition states. *J. Am. Chem Soc.* **1999**, *121*, 3933−3938
(15) Smith, L. E. H.; Mohr, L. H.; Raftery, M. A. Mechanisms for lysozyme-catalyzed hydrolysis. *J. Am. Chem. Soc.* **1973**, *95*, 7497.
(16) Rodgers, J.; Femec, D. A.; Schowen, R. L. Isotopic mapping of transition-state structural features associated with enzymatic catalysis of methyl transfer. *J. Am. Chem. Soc.* **1982**, *104*, 3263.
(17) Sicinska, D.; Truhlar, D. G.; Paneth, P.; Solvent-dependent transition states for decarboxylations. *J. Am. Chem. Soc.* **2001**, *123*, 7683−7686.
(18) Bruice, T. C.; Lightstone, F. C. Ground state and transition state contributions to the rates of intramolecular and enzymatic reactions. *Acc. Chem. Res.* **1999**, *32*, 127−136
(19) Matthews, D. A.; Bolin, J. T.; Burridge, J. M.; Filman, D. J.; Volz, K. W.; Kaufman, B. T.; Beddell, C. R.; Champress, J. N.; Stammers, D. K.; Kraut, J. Dihydrofolate reductase. The stereochemistry of inhibitor selectivity. *J. Biol. Chem.* **1985**, *260*, 381−391.
(20) Merkler, D. J.; Kline, P. C.; Weiss, P.; Schramm, V. L. Transition state analysis of AMP deaminase. *Biochemistry* **1993**, *32*, 12993−13001.
(21) Lewandowicz, A.; Rudzinski, J.; Luo, L.; Dunaway-Mariano, D.; Paneth, P. Determination of the chlorine kinetic isotope effect on the 4-chlorobenzoyl-CoA dehalogenase-catalyzed nucleophilic aromatic substitution. *Arch. Biochem. Biophys.* **2002**, *398*, 249−252.
(22) Chen, X.-Y.; Link, T. M.; Schramm, V. L. Inhibition of ricin by an RNA stem-loop containing a rib-oxycarbonium mimic. *J. Am. Chem. Soc.* **1996**, *118*, 3067−3068.
(23) Chen, X.-Y.; Berti, P. J.; Schramm, V. L. Transition state structure for depurination of DNA by ricin A-chain. *J. Am. Chem. Soc.* **2000**, *122*, 6527−6534.
(24) Werner, R. M.; Stivers, J. T. Kinetic isotope effect studies of the reaction catalyzed by uracil DNA glycosylase: Evidence for an oxocarbenium ion-uracil anion intermediate. *Biochemistry* **2000**, *39,* 14054−14064.
(25) Amyes, T. L.; Jencks, W. P. Lifetimes of oxocarbenium ions in aqueous solution from common ion inhibition of the solvolysis of.alpha.-azido ethers by added azide ion. *J. Am. Chem. Soc.* **1989**, *111*, 7888−7900.
(26) Parikh, S. S.; Walcher, G.; Jones, G. D.; Slupphaug, G.; Krokan, H. E.; Blackburn, G. M.; Tainer, J. A. Uracil-DNA glycosylase-DNA substrate and product structures: Conformational strain promotes catalytic efficiency by coupled stereoelectronic effects. *Proc. Nat. Acad. Sci. U.S.A.* **2000**, *97*, 5083−5088.
(27) Chen, X.-Y.; Link, T. M.; Schramm, V. L. Ricin A-chain: kinetics, mechanism and RNA-stem-loop inhibitors. *Biochemistry* **1998**, *37*, 11605−11613.
(28) Tanaka, K. S. E.; Chen, X.-Y.; Ichikawa, Y.; Tyler, P. C.; Furneaux, R. H.; Schramm, V. L. Ricin A-chain inhibitors resembling the oxacarbenium ion transition state. *Biochemistry* **2001**, *40*, 6845−6851.
(29) Kati, W. M.; Acheson, S. A.; Wolfenden, R. A transition state in pieces: major contributions of entropic effects to ligand binding by adenosine deaminase. *Biochemistry* **1992**, *31*, 7356−7366.
(30) Mazzella, L. J.; Parkin, D. W.; Tyler, P. C.; Furneaux, R. H.; Schramm, V. L. Mechanistic diagnoses of N-ribohydrolases and purine nucleoside phosphorylase. *J. Am. Chem. Soc.* **1996**, *118*, 2111−2112.
(31) Jiang, Y. L.; Stivers, J. T. Mutational analysis of the base-flipping mechanism of uracil DNA glycosylase. *Biochemistry* **2002**, *41*, 11236−11247.
(32) Jiang, Y. L.; Ichikawa, Y.; Stivers, J. T. Inhibition of uracil DNA glycosylase by an oxacarbenium ion mimic. *Biochemistry* **2002**, *41*, 7116−7124.
(33) Parkin, D. W.; Horenstein, B. A.; Abdulah, D. R.; Estupinan, B.; Schramm, V. L. Nucleoside hydrolase from *Crithidia fasciculata.* Metabolic role, purification, specificity, and kinetic mechanism. *J. Biol. Chem.* **1991**, *266*, 20658−20665.
(34) Dai, Y.; Pochapsky, T. C.; Abeles, R. H. Mechanistic studies of two dioxygenases in the methionine salvage pathway of *Klebsiella pneumoniae. Biochemistry* **2001**, *40*, 6379−6387.
(35) Winzer, K.; Hardie, K. R.; Burgess, N.; Doherty, N.; Kirke, D.; Golden, M. T. G.; Linforth, R.; Cornell, K. A.; Taylor, A. J.; Hill, P. J.; Williams, P.; Lux, S. its role in central metabolism and the in vitro synthesis of 4-hydroxy-5-methyl-3(2H)-furanone. *Microbiology* **2002**, *148*, 909−922.

(36) Horenstein, B. A.; Parkin, D. W.; Estupinan, B.; Schramm, V. L. Transition state analysis of nucleoside hydrolase from *Crithidia fasciculata*. *Biochemistry* **1991**, *30*, 10788−10795.
(37) Parkin, D. W.; Limberg, G.; Tyler, P. C.; Furneaux, R. H.; Chen, X.-Y.; Schramm, V. L. Isozyme-specific transition state inhibitors for the trypanosomal nucleoside hydrolases. *Biochemistry* **1997**, *36*, 3528−3534.
(38) Parkin, D. W. Purine-specific nucleoside N-ribohydrolase from *Trypanosoma brucei brucei*. *J. Biol. Chem.* **1996**, *271*, 21713−21719.
(39) Giblett, E. R.; Ammann, A. J.; Wara, D. W.; Sandman, R.,; and Diamond, L. K. Nucleoside-phosphorylase deficiency in a child with severely defective T-cell immunity and normal B-cell immunity. *Lancet* **1975**, *1,* 1010−1013.
(40) Kicska, G. A.; Long, L.; Hörig, H.; Fairchild, C.; Tyler, P. C.; Furneaux, R. H.; Schramm, V. L.; Kaufman, H. L. Immucillin-H a powerful transition state analogue inhibitor of purine nucleoside phosphorylase, selectively inhibits human T-lymphocytes. *Proc. Natl. Acad. Sci. U.S.A.* **2001**, *98*, 4593−4598.
(41) Kline, P. C.; Schramm, V. L. Purine nucleoside phosphorylase. Catalytic mechanism and transition state analysis of the arsenolysis reaction. *Biochemistry* **1993**, *32*, 13212−13219.
(42) Kline, P. C.; Schramm, V. L. Purine nucleoside phosphorylase. Inosine hydrolysis, tight binding of the hypoxanthine intermediate and third-the-sites reactivity. *Biochemistry* **1992**, *31*, 5964−5973.
(43) Miles, R. W.; Tyler, P. C.; Furneaux, R. H.; Bagdassarian, C. K.; Schramm, V. L. One-third-the-sites transition state inhibitors for purine nucleoside phosphorylase. *Biochemistry* **1998**, *37*, 8615−8621.
(44) Fedorov, A.; Shi, W.; Kicska, G.; Fedorov, E.; Tyler, P. C.; Furneaux, R. H.; Hanson, J. C.; Gainsford, G. J.; Larese, J. Z.; Schramm, V. L.; Almo, S. C. Transition state structure of purine nucleoside phosphorylase and principles of atomic motion in enzymatic catalysis. *Biochemistry* **2001**, *40*, 853−860.
(45) Garrett, E. R.; Mehta, P. J. Solvolysis of adenine nucleosides. I. Effects of sugars and adenine substituents on acid solvolysis. *J. Am. Chem. Soc.* **1972**, *94*, 8532−8541.
(46) McCarter, J. D.; Withers, S. G. Mechanisms of enzymatic glycoside hydrolysis. *Curr. Opin. Struct. Biol.* **1994**, *4*, 885−892.
(47) Vocadlo, D. J.; Davies, G. J.; Laine, R.; Withers, S. G. Catalysis by hen egg-white lysozyme proceeds via a covalent intermediate. *Nature* **2001**, *412*, 835−838.
(48) Kicska, G. A.; Tyler, P. C.; Evans, G. B.; Furneaux, R. H.; Shi, W.; Fedorov, A., Lewandowicz, A.; Cahill, S. M.; Almo, S. C.; Schramm, V. L. Atomic dissection of the hydrogen bond network for transition state analogue binding to purine nucleoside phosphorylase. *Biochemistry* **2002**, *41*, 14489−14498.
(49) Mazumder, D.; Bruice, T. C. Exploring nucleoside hydrolase catalysis in silico: molecular dynamics study of enzyme-bound substrate and transition state. *J. Am. Chem. Soc.* **2002**, *124*, 14591−14600.
(50) Sauve, A. A.; Cahill, S. M.; Zech, S. G.; Basso, L. A.; Santos, D. S.; Grubmeyer, C.; Evans, G. B.; Furneaux, R. H.; Tyler, P. C.; McDermott, A.; Girvin, M. E.; Schramm, V. L. Ionic states of substrates and transition state analogues at the catalytic sites of N-ribosyltransferases. *Biochemistry* **2003**, in press.
(51) Scheuring, J.; Schramm, V. L. Kinetic isotope effect characterization of the transition state for oxidized nicotinamide adenine dinucleotide hydrolysis by pertussis toxin. *Biochemistry* **1997**, *36*, 4526−4534.
(52) Scheuring, J.; Schramm, V. L. Pertussis toxin: transition state analysis for ADP-ribosylation of G-protein peptide $_{\alpha i3}$C20. *Biochemistry* **1997**, *36*, 8215−8223.
(53) Scheuring, J.; Berti, P. J.; Schramm, V. L. Transition-state structure for the ADP-ribosylation of $G_{i\alpha 1}$ subunits by pertussis toxin. *Biochemistry* **1998**, *37*, 2746−2758.
(54) Markham, G. D.; Parkin, D. W.; Mentch, F.; Schramm, V. L. A kinetic isotope effect study and transition state analysis of the S-adenosylmethionine synthetase reaction. *J. Biol. Chem.* **1987,** *262*, 5609−5615.
(55) Lewandowicz, A.; Sicinska, D.; Rudzinski, J.; Ichiyama, S.; Kurihara, T.; Esaki, N.; Paneth, P. Chlorine kinetic isotope effect on the fluoroacetate dehalogenase reaction. *J. Am. Chem. Soc.* **2001**, *123*, 9192−9193.
(56) Lewandowicz, A.; Rudzinski, J.; Tronstad, L.; Widersten, M.; Ryberg, P.; Matsson, O.; Paneth, P. Chlorine kinetic isotope effects on the haloalkane dehalogenase reaction. *J. Am. Chem. Soc.* **2001**, *123*, 4550−4555.
(57) Schramm, V. L. Enzymatic transition-state analysis and transition-state analogues. *Methods Enzymol.* **1999**, *308*, 301−355.
(58) Lewandowicz, A.; Shi, W.; Evans, G. B.; Tyler, P. C.; Furneaux, R. H.; Basso, L. A.; Santos, D. S.; Almo, S. C.; Schramm, V. L. Over-the-barrier transition state analogues and crystal structure with *Mycobacterium tuberculosis* purine nucleoside phosphorylase. *Biochemistry*, in press.

AR0200495